

Strengthening of Reinforced Concrete Beams in Flexural Zone Using Different Materials: an experimental and numerical study

Waleed Hamed Kamel¹ Bilal Ismaeel Abd Al-Zahra²

¹ Civil Engineering, College of Engineering, University of Babylon, Hilla, Babylon, Iraq.
ORCID: 0009-0007-4682-4012

waleed.omran.engh323@studen.uobabylon.edu.iq

² College of Engineering, University of Babylon, Hilla, Babylon, Iraq. ORCID: 000-0001-8275-2924

eng.bilal.ismaeel@uobabylon.edu.iq

Received: 21/1/2024 **Accepted:** 3/3/2024 **Published:** 24/6/2024

Abstract

Beams that crack are thought to be strengthened faster by using strengthening materials. The purpose of this study is to investigate how Ultra-High-Performance Concrete (R-UHPC), Basalt Fiber Reinforced Polymer (BFRP), and Near Surface Mounted Glass Fiber Reinforced Polymer bar (NSM-GFRP) behave in simply supported strengthened concrete. To complete this study, four beams had to be prepared, cast, and tested. Where one of the beams was adopted as a control beam, and the remaining three beams were strengthened with three different types of strengthen that will be explained later. One of the study's variables is the strengthening shape or type. To test the specimens, the specific technique applied a two-point load. By talking about the ultimate load, method of failure, cracking development, and load-deflection response, the structural behavior of the specimens was studied. The results of the study illustrated that, in comparison to the control and strengthened specimens, the specimen strengthened with R-UHPC given great increase in ultimate load. Where, the ultimate load is improved by 143% in R-UHPC specimens, 32.5% in BFRP specimens, and 91.01% in NSM-GFRP specimens when strengthening is present. Additionally, strengthened specimens were able to absorb more energy than unstrengthen specimens. Additionally, a numerical analysis using ABAQUS was carried out on the anticipated model that replicated the experimentally tested beams. The load-deflection response and mechanism of failure show that the F.E. model's results and the laboratory test agreed well.

Key word: Strengthening, BFRP, R-UHPC, and NSM-GFRP.

1. Introduction

Various materials can be used to strengthen reinforced concrete beams in the flexural zone, one of which being Near Surface Mounted Glass Fiber Reinforced Polymer bar (NSM-GFRP), Ultra-High-Performance Concrete (UHPC), and Basalt Fiber Reinforced Polymer (BFRP). Each material has special characteristics and advantages, and the choice of material depends on the project's specific specifications.

BFRP, a composite material that is comparable to CFRP but uses basalt fibers in place of carbon fibers, exhibits notable tensile strength, corrosion resistance, and fire resistance [1]. A

study conducted by Mr. Ankit et al. in 2017 [2] showed that adding more basalt fiber weave layers to beams significantly increased their load-bearing capacity. Additionally, Harshwardhan et al. in 2019 [3] observed an enhanced maximum load capacity in all retrofitted beams compared to the control beam. While study by Viswanathan et al. in 2019 [4] highlighted the achievement of the maximum bending resistance in beams reinforced with basalt fiber.

Ultra-high-performance concrete, or UHPC, is a composite material based on cementitious technology that offers several advantages over traditional materials. UHPC is characterized by its remarkable endurance and improved mechanical qualities, which include a minimum compressive strength of 120 MPa [5],[6]. It is usually composed of a compact blend of cement, tiny particles, fibers (such steel or synthetic fibers), and chemical additives. In the flexural portion of reinforced concrete beams, UHPC is used as an enclosing material to increase the strength and durability of the beam or as a replacement for concrete that has deteriorated [7]. Because of factors like steel fibers, low free water content, and low permeability, UHPC stands out from normal concrete in that it shrinkage less than the latter [8],[9].

The process of inserting NSM-GFRP is the term for glass fiber reinforced polymer (GFRP) bars or rods inserted into carved slots or grooves in the concrete surface close to a beam's tension side, or Near-Surface-Mounted Glass Fiber Reinforced Polymer. The load-bearing capacity of current reinforced concrete beams can be increased with the help of this strengthening technique[10]. According to research done by W. C. Tang et al. in 2005 [11] beams using NSM GFRP bars showed improvements in bending capacity and flexural stiffness but lower ultimate deflection. Roberto in 2014 [10] highlighted the importance of pull-out testing, showing that until the rod's tensile strength is exceeded, the link between the GFRP rod, resin, and concrete is maintained. For comparison, Reda et al. in 2016 [12] used straight GFRP bars of different lengths in addition to GFRP bars with bent ends positioned at 90 and 45 degrees. The results of the tests showed that GFRP bars with bent ends significantly increased the reinforced beams' ability to support loads and prevented the concrete cover from separating.

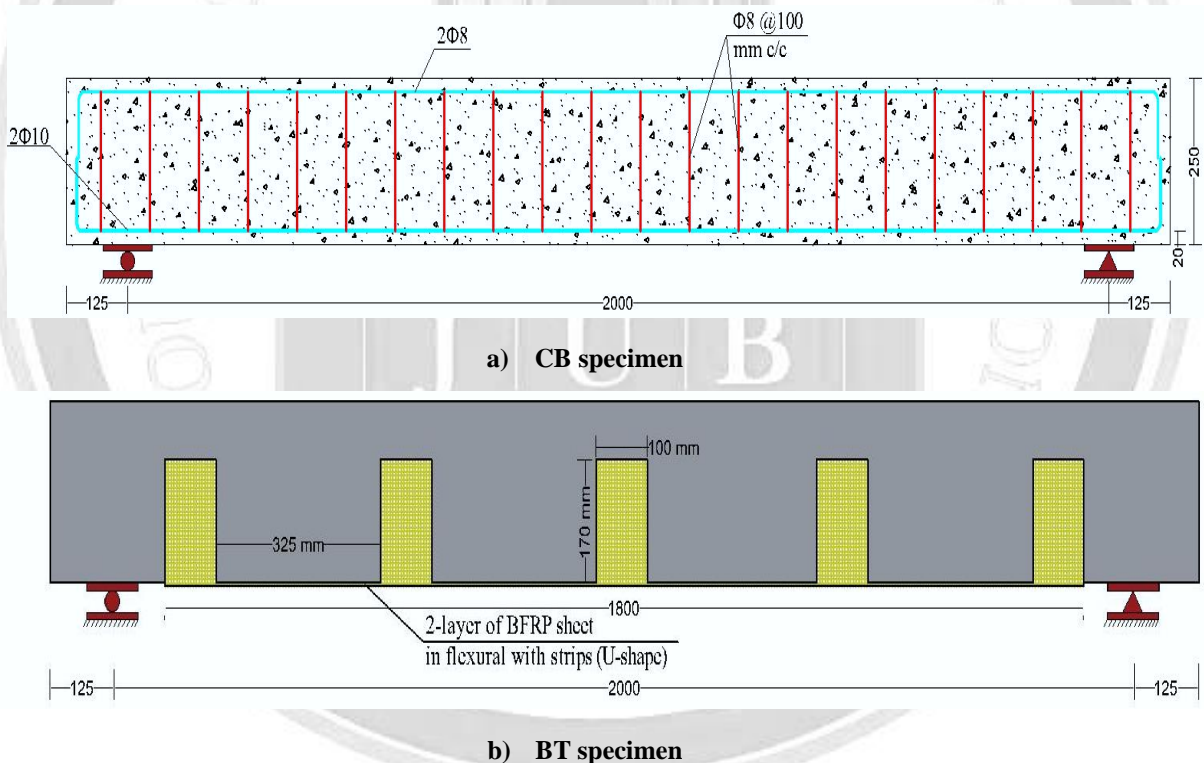
Many considerations, including as the necessary load-carrying capability, durability, compatibility with pre-existing materials, installation requirements, and cost-effectiveness, are taken into account when choosing appropriate materials for strengthening reinforced concrete beams [13]. The main aims of this study are:

- 1- Experimental investigation of the ultimate strength, cracking load, cracking patterns, modes of failure, lateral and axial displacement, concrete strain of repaired reinforced concrete beams.
- 2- Investigating experimentally, the improvement that provided by strengthened Reinforced Ultra High-Performance Concrete (R-UHPC), Basal Fiber Reinforced Polymer sheet (BFRP), and Near-Surface Mounted Glass Fiber Reinforced Polymer Bar (NSM GFRP) on reinforced concrete beams subjected to external load.
- 4- Numerical study by F.E.M analysis by using ABAQUS computer program and comparing the results with those obtained experimentally.

2. Experimental Project

2.1 Study materials

The test specimens were designed in accordance with the guidelines supplied by the American Concrete Institute (ACI-318-19) [14] and were built using the testing apparatus that was available and its capacity. Each of the test samples had the same dimensions: a total depth of 250 mm, a width of 150 mm, and a clear span of 2000 mm, as shown in Fig. 1. 2 Φ 10 mm at the bottom, 2 Φ 8 mm at the top, and Φ 8@100 mm for shear reinforcement were used to reinforce each girder. Furthermore, each beam included a 20 mm clear cover at all sides to guarantee flexural failure. The testing matrix for the specimens is presented in Table 1. The first specimen, designated as (CB), is a control specimen that is represented by a beam composed of normal-strength concrete (NSC), as seen in Fig. 1a. The remaining three specimens were identified as follows: NSM-GFRP bar of 1 ϕ 16mm along 1800 mm of the beam length symbolized by (NGb), strengthened with two layers of BFRP sheets symbolized by (BT), and strengthened with (50 mm) of R-UHPC bonded in a U-shape along 1800 mm of the beam length symbolized by (RU).



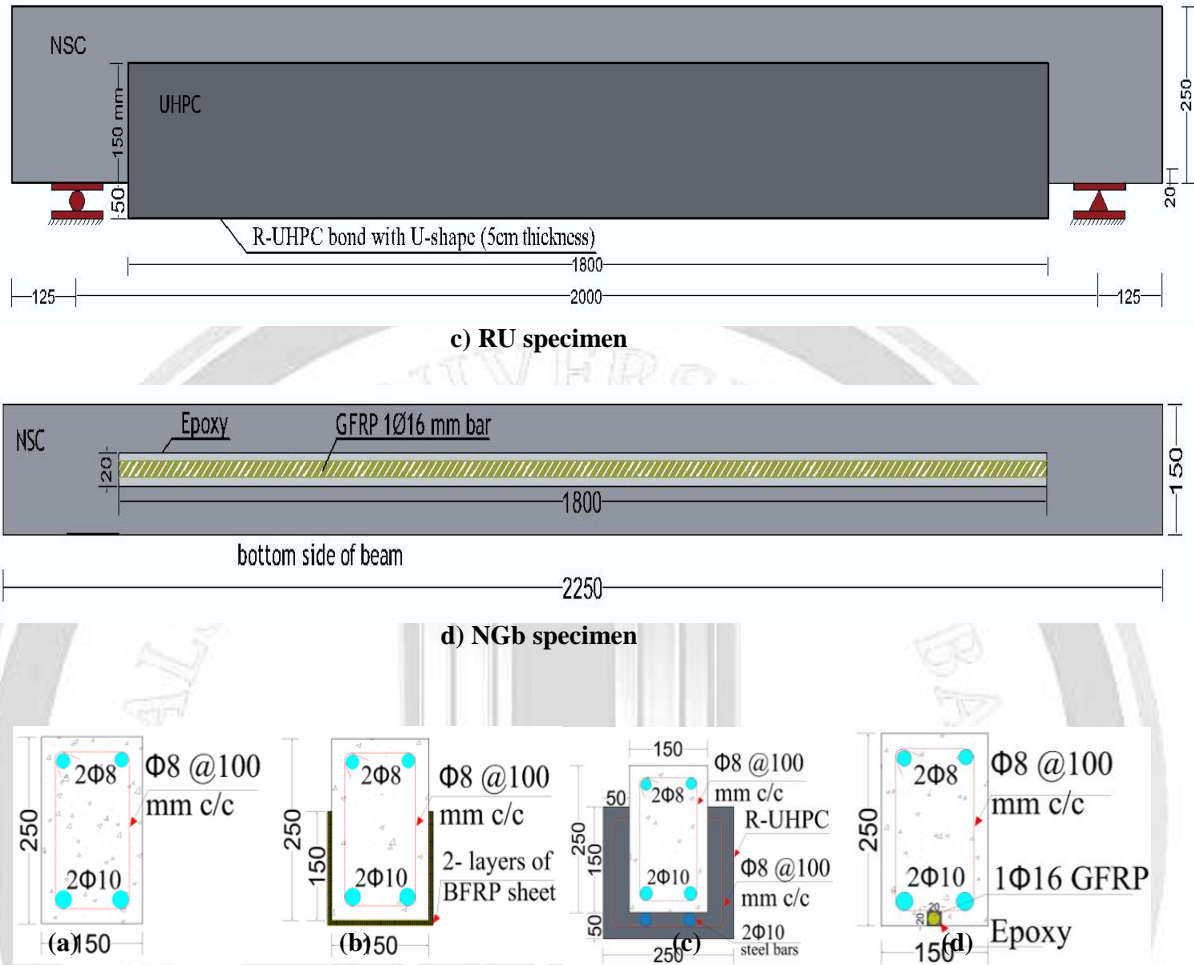


Figure 1: Detail of specimens and manufacturing procedure.

Table 1: provides an overview of the characteristics of the specimens prepared for testing.

Specimen	Specimen Type	Type of Material (strengthening or repairing)	Processing Type	Strengthening or Repairing Length (mm)
CB	control	-	-	-
BT	2-layers external bond sheet only	BFRP	Strengthen	1800
RU	R-UHPC bond with U-shape only with (50 mm thickness)	R-UHPC	Strengthen	1800
NGb	NSM -GFRP bar 1Ø16mm only	GFRP	Strengthen	1800

2.2 Proportions of mixtures and material qualities:

In this investigation, a mixture of components listed in Table 2 was used to create Ultra-High-Performance Concrete (UHPC). The fine aggregate in the mix design was fine sand with particles smaller than 0.6 mm, and the binding agents were silica fume and Portland cement. In addition to adding 3% superplasticizer (SP) to enhance flowability, 2% micro steel fiber was utilized to strengthen the UHPC matrix. The intended compressive strength of the ready-mix utilized in the casting of the Non-Structural Concrete (NSC) components was roughly 30 MPa. While Table 3 provides data on the mechanical parameters of the steel bar, Table 4 provides an overview of the material qualities of the generated UHPC and NSC. Six cube specimens, each with side lengths of 50 mm, underwent compressive strength testing. The cube results closely aligned with the cylinder results, as per the ASTM standard (ASTM C1856, 2017) [15], corroborated by studies conducted by Yuliarti et al. in 2015 [16], Graybeal and Davis in 2008 [17], and Aziz and Ahmed in 2012 [18]. Furthermore, indirect tensile stress was measured following ASTM C469-11 (2008) [19]. The modulus of elasticity for UHPC was calculated using the recommended equation (Eq. (1)) [19], while the modulus of elasticity for NSC was computed using (Eq. (2)) (ACI-318, 2019) [14].

Table 2: Proportion of Mix for UHPC

Mixture	Cement	Fine Sand	Silica Fume	Water	S.P.	Steel Fiber
UHPC (Kg/m ³)	950	1050	190 ^a	178.7 ^b	39.9 ^c	157 ^d

^a silica =0.20 of cement weight, ^b w/b =0.155, ^c S.P./b=0.03 and ^d steel fibre=0.02 of total volume [20].

Table 3: Steel reinforcing bar specifications and test outcomes.

Diameter as Nominal (mm)	Diameter as Measured (mm)	Stress of Yield (MPa)	Ultimate strength (MPa)
10.00	9.95	560	602
8.00	8.01	565	706

Table 4: Material Characteristics of UHPC and NSC

Type of Concrete	f_{cu} (MPa)	f_t (MPa)	E_c (GPa)
NSC.	32.41	3.24	25.743
UHPC.	132.02	13.20	44.118

f_{cu} : reflects the compressive strength, which was established by testing six cubic and 150 mm × 300 mm cylinder specimens, for UHPC and NSC respectively.

f_t : signifies the indirect tensile strength (splitting), evaluated with three 100 mm × 200 mm cylinder specimens for both UHPC and NSC.

The modulus of elasticity (E) for NSC is calculated as $E_c = 4700 \sqrt{f_c}$ (MPa) (1)

And the modulus of elasticity (E) for NSC is calculated as $E_c = 3840 \sqrt{f_c}$ (MPa) (2)

UHPC samples undergo reinforcement by drilling holes at both sides and the bottom using drilling equipment. Subsequently, the holes are washed with water and cleaned using compressed air to eliminate dust, enhancing the bonding process. Following this, additional main reinforcement of 210 mm and 8 @ 100 mm stirrups are introduced externally along an 1800 mm span at the bottom of the beam. Refer to Figure (2) for a visual representation of this process.



Fig. 2: Steps of reinforced beam for UHPC and mixing procedure.

Cut the BFRP sheet to the specified length and ensure thorough cleaning of the concrete surface. Additionally, reinforce the specimen with a $1\phi 16$ mm near-surface-mounted glass fiber-reinforced polymer bar. To create grooves, utilize a diamond cutter with dimensions of 20 mm in width and 20 mm in depth on the concrete cover. Subsequently, wash the grooves with water and use compressed air to eliminate dust, ensuring optimal bonding conditions (Sami H. Rizkalla Chai, 2004) [21]. In a 4:1 ratio, mix two distinct types of epoxies (A and B) adhesive (Sikadur-330) until the color is uniform. That epoxy was utilized to attach BFRP sheets or GFRP bars to beams. Figure (3) depicts this.



Fig. 3: Steps of applying BFRP sheets and NSM-GFRP bar.

2.3 Tools and Testing

The instrumentation and setup of the test specimens are shown in Figure (4). The beams were put through failure tests with a two-point loading configuration after being strengthened using three distinct techniques involving the application of BFRP sheets, R-UHPC (U-warp), and NSM-GFRP bars.

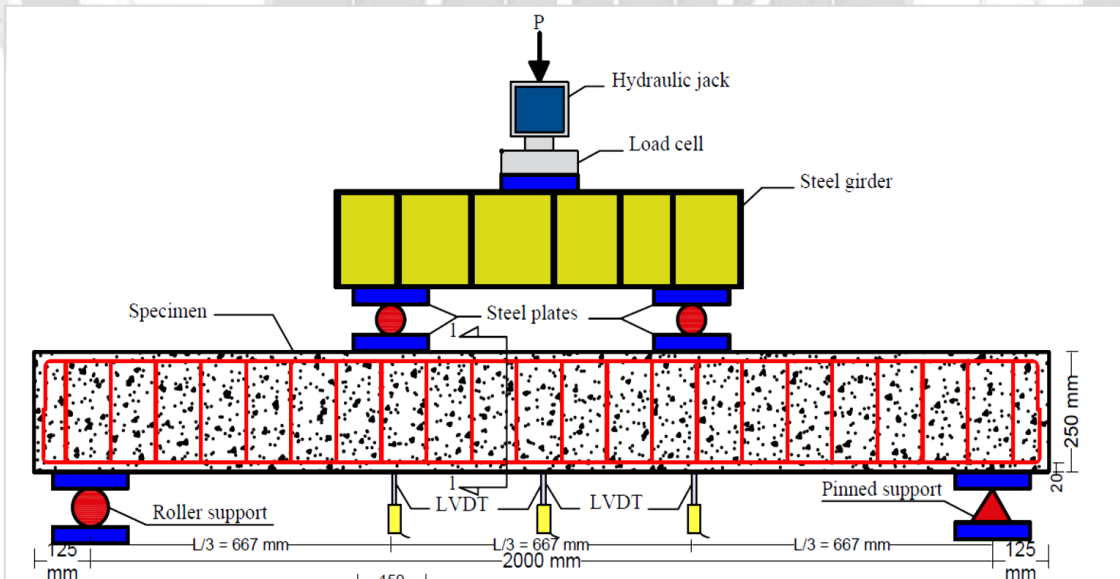


Fig. 4: Specimen instrumentation and testing setup.

3. Test results and conversation

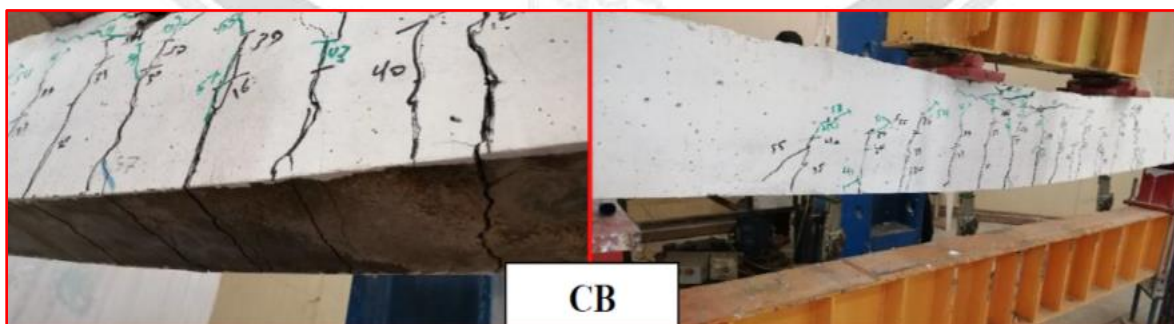
3.1 The method of failure and crack pattern

According to the design specifications, all beams exhibit flexural fractures in the mid-span zone as they get closer to a certain failure stress caused by flexural strains. At a load of 15 kN, the control specimen's midspan experiences the first crack, which is thereafter exacerbated at the prescribed rate. At this stage, the beam develops extensive cracks in the midspan zone, leading to flexural failure at 59.12 kN. The first cracks emerge at the midspan of specimens (BT, RU, and NGb) at loads of 15, 42, and 15 kN, respectively. At this juncture, the beams exhibit numerous vertical cracks in the central section with varying crack widths, and the extensive nature of the cracks extends to the top, resulting in failure at (BT at 78.34 kN, RU at 143.65 kN, and NGb at 112.93 kN). Refer to Table (5) for details.

Table 5: Summary of test results.

Beams Symbol	First crack Load Pcr (KN)	Load Carrying Capacity Pu (kN)	Ultimate mid-span Deflection (mm)	Crack width (First crack at ultimate load) (mm)	Failure mode
CB	15	59.12	29.82	3.2	Typical flexural failure
BT	15	78.34	18.32	2.6	Rupture of BFRP sheet
RU	42	143.65	17.18	1.5	De-ponding between UHPC and old concrete
NGb	15	112.93	18.74	2.6	Concrete cover separation

The reinforcement led to a reduction in deflection for the specimens (from 29.28 to 18.32, 17.18, and 18.74 mm) for beams directly reinforced by (BT, RU, and NGb) respectively. The mode of failure and crack patterns for each specimen are illustrated in Figure (5).



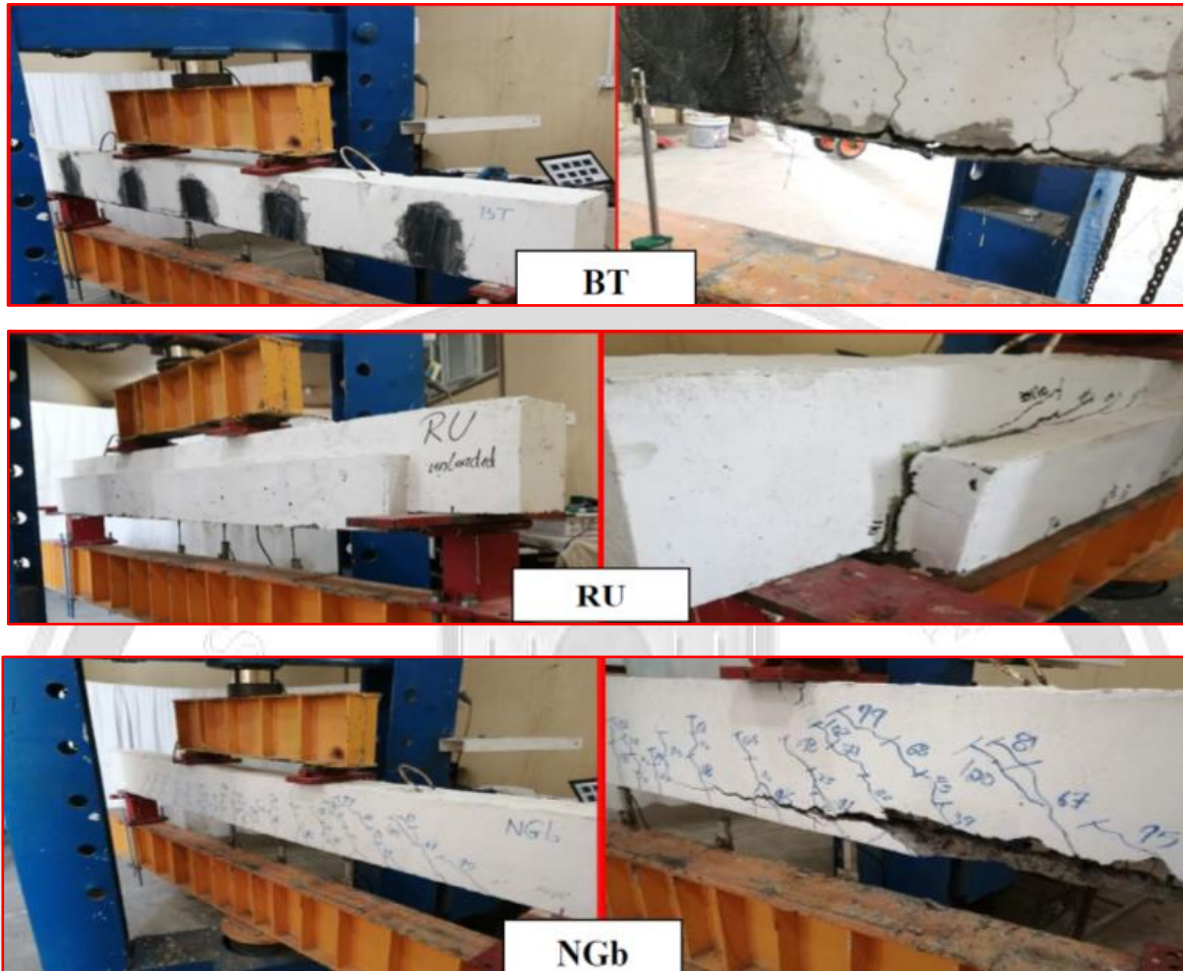
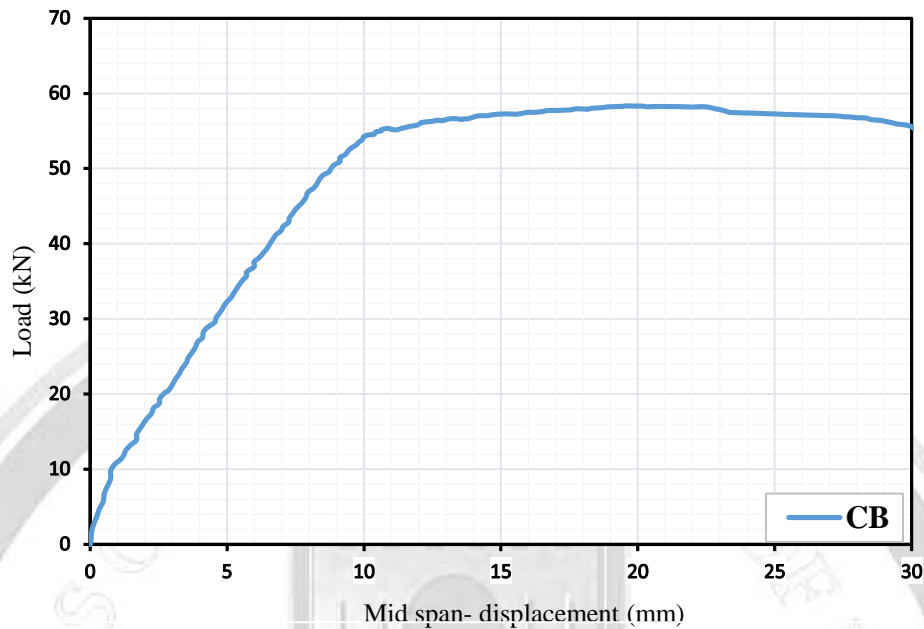


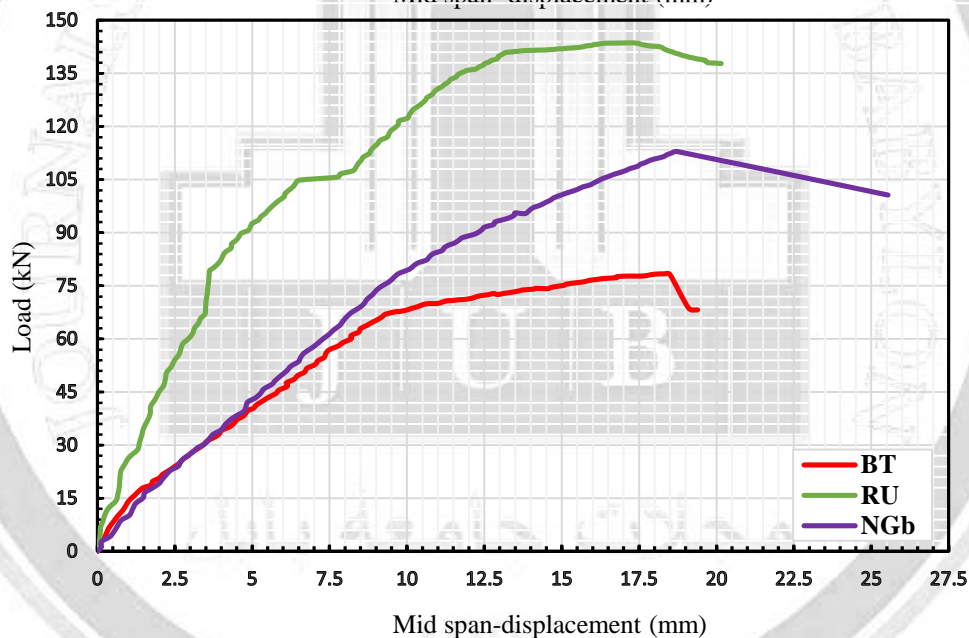
Fig. 5: Mode of failure and cracks separations.

3.2 Relationship between load and deflection

Figure 6 (a and b) illustrates the load-deflection responses in the midspan region of all tested specimens. Prior to the occurrence of flexural cracking, a linear load-deflection response was observed in all specimens. Subsequently, variations in beam yielding stages became apparent, with beam BT exhibiting a lower yield load, and beam RU showing a higher yield load. Leading up to the collapse stage, all beams exhibited good ductile responses. Because of the strong connection between the UHPC jacket and precast beams, the load-deflection responses of the beams enhanced with UHPC were comparable. Notably, the load capacity significantly increased as a percentage, with strengthened beams (BFRP, R-UHPC, and NSM-GFRP) experiencing load increases of (32%, 143%, and 95%), respectively, compared to the control beam. The results highlight a notably higher percentage improvement in loading capacity for beams strengthened with R-UHPC compared to beams strengthened with other materials.



(a)



(b)

Fig. 6: Load-midspan deflection responses.

4. Analysis using numerals

The Finite Element Method (FEM) in ABAQUS was used to numerically simulate the RC beams corresponding to CB, BT, RU, and NGb. The original finite element model and the experimental test results were compared to verify the efficacy of the FEM analysis. Based on stress-strain characteristics, all material behaviors that were necessary for the simulation were directly included into the models that were chosen. The elastic-perfect plastic model was used to model the reinforcement, and an elastic model was used to simulate the plate load and support. A three-dimensional eight-nodes linear brick element (C3D8R) with limited

integration hourglass control was utilized to represent the concrete, plate load, and plate support. A two-nodes element (T3D2: a 2-noded linear 3-D truss element type) was employed for reinforcement, as shown in Fig. 7. Moreover, a mesh sensitivity analysis was carried out to determine the optimal node density (or element size) for the simulation process. Using five alternative mesh sizes, the mesh sensitivity analysis for the control girder was carried out under monotonic loads, as shown in Fig. (8), in order to determine the most effective mesh arrangement with the least amount of computational time. An element size of 20 mm was chosen for this experiment in order to balance computational efficiency and accuracy.

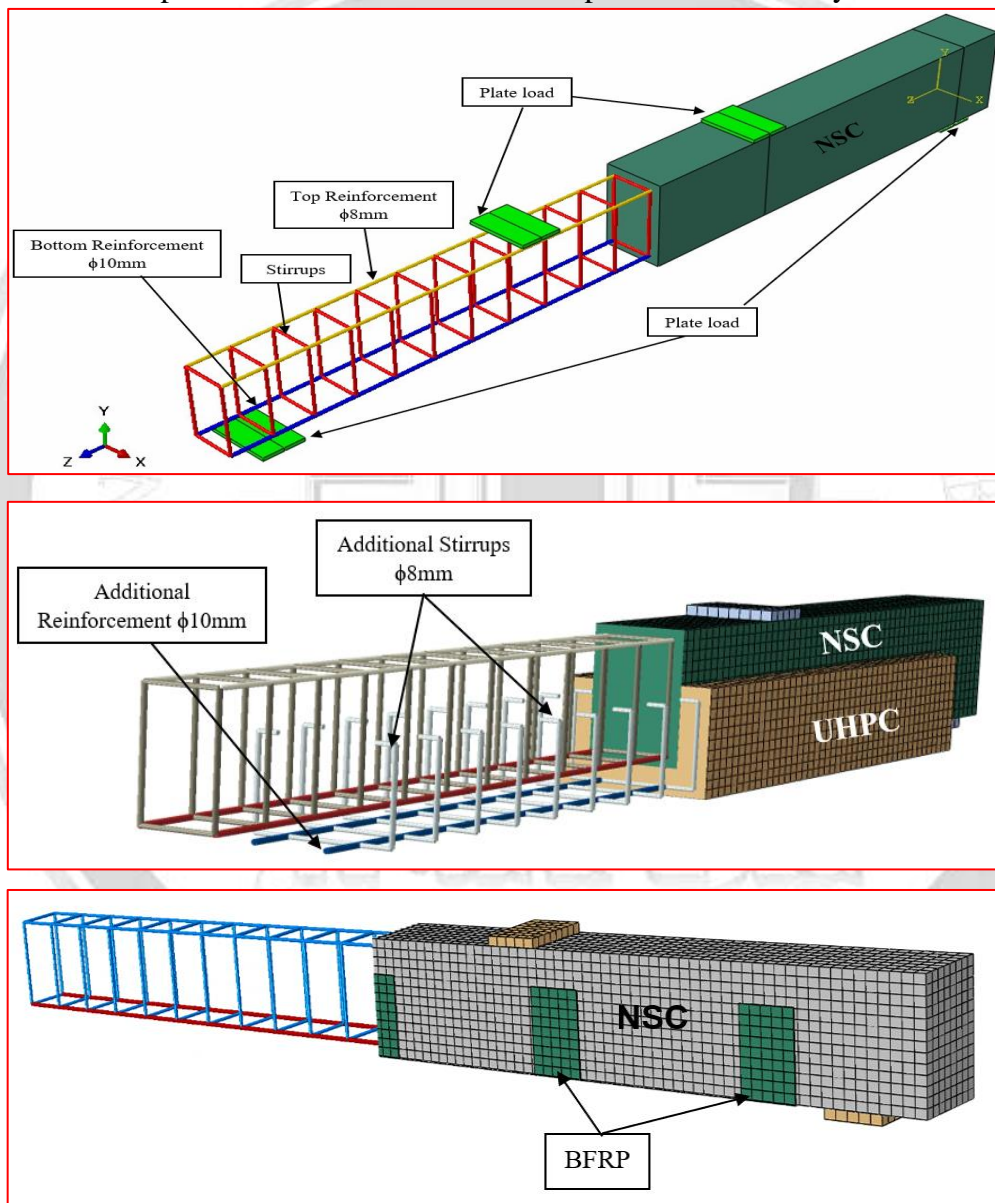


Fig. 7: An explanation of the components used in the model.

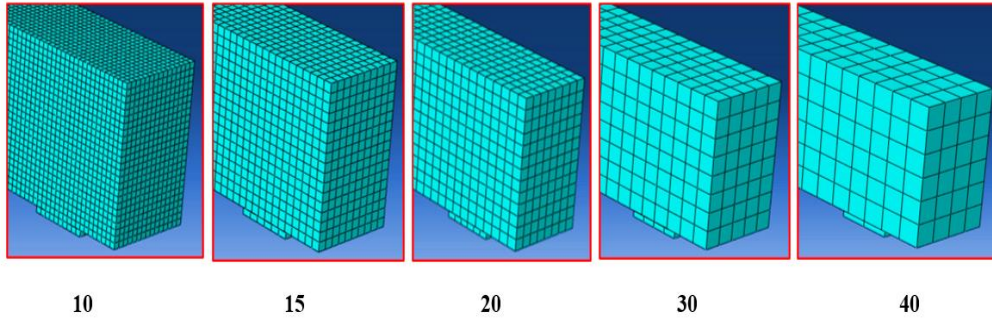


Fig. 8: The tested mesh sizes.

To capture both the elastic and plastic phases of concrete, the Concrete Damaged Plasticity (CDP) model was utilized. Table 6 outlines the essential parameters needed for the CDP model to represent the elastic phase of concrete. The plastic phase necessitates the inclusion of compression and tension behaviors, along with the incorporation of damage parameters. For NSC, the predictive formulas proposed by Wang and Hsu in 2001 [22] were employed for compression (Eqs. (3), (4), (5), and (6)) and tension (Eqs. (7), (8), and (9)), as illustrated in Fig. 9.

Table 6: The parameters used in CDP model of concrete

Parameters	NSC
E_c	25,743 MPa
Poisson's ratio	0.2
Dilation Angle*	30
Eccentricity	0.1
f_{b0}/f_{c0}	1.16
K_c	0.667
Viscosity*	0.00001

*Calibrated value

$$\sigma_c = \xi f_c \left[2 \left(\frac{\varepsilon_{cu}}{\xi \varepsilon_{c1}} \right) - \left(\frac{\varepsilon_{cu}}{\xi \varepsilon_{c1}} \right)^2 \right] \quad \text{if } \frac{\varepsilon_{cu}}{\xi \varepsilon_{c1}} \leq 1 \quad (3)$$

$$\sigma_c = \xi f_c \left[1 - \left(\frac{\frac{\varepsilon_{cu}-1}{\xi \varepsilon_{c1}}}{\frac{\xi}{2}-1} \right)^2 \right] \quad \text{if } \frac{\varepsilon_{cu}}{\xi \varepsilon_{c1}} > 1 \quad (4)$$

$$\varepsilon_{c1} = 0.0014 \xi f_c [2 - \exp(-0.024f_c) - \exp(-0.14f_c)] \quad (5)$$

$$\varepsilon_{cu} = 0.004 - 0.0011 [1 - \exp(-0.0215f_c)] \quad (6)$$

Here, the symbol ξ denotes the compressive stress reduction coefficient, set at 1. The variables f_c , ε_{c1} , and ε_{cu} indicates the concrete's ultimate strain, its strain at maximum compressive stress, and its cylinder compressive strength, respectively.

$$\sigma_t = E_c \varepsilon_t \quad \text{if } \varepsilon_t \leq \varepsilon_{cr} \quad (7)$$

$$\sigma_t = f_{cr} \left(\frac{\varepsilon_{cr}}{\varepsilon_t} \right)^{0.4} \quad \text{if } \varepsilon_t > \varepsilon_{cr} \quad (8)$$

And

$$f_{cr} = 0.31 \sqrt{f_c} \text{ (MPa)} \quad (9)$$

Here, E_c represents the modulus of elasticity of concrete, f_{cr} denotes the cracking stress of concrete, and ε_{cr} stands for the cracking strain of concrete, assumed to be 0.00008, while ε_t represents the tension strain.

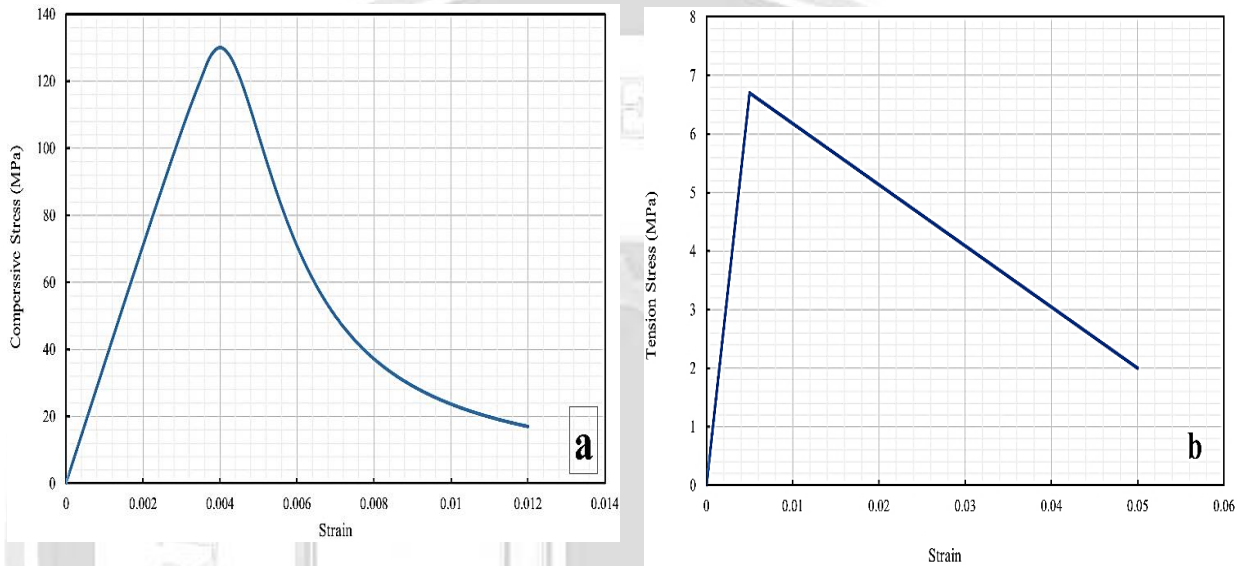


Fig. 9: The stress strain curve of NSC with $f_c = 30$ MPa, (a) in compression and (b) in tension.

For UHPC, the stress-strain data obtained follow the formulation outlined by Russell et al. in 2013 [23] for compression (Equations (10), (11), and (12)) and tension (Equation (13)), as illustrated in Figure 10.

$$\sigma_c = E_c \varepsilon_c \text{ if } \sigma_c \leq 0.5 f_c \quad (10)$$

$$\sigma_c = E_c \varepsilon_c (1 - \alpha) \text{ if } \sigma_c > 0.5 f_c \quad (11)$$

And

$$\alpha = \left(0.001 * e^{\frac{E_c \varepsilon_c}{0.243 * f_c}} \right) - 0.001 \quad (12)$$

where: σ_c represents compressive stress; ε_c signifies concrete strain; α denotes a coefficient reflecting the deviation of the actual stress–strain curve from the linear trend.

$$\sigma_t = 0.55 \sqrt{f_c} \text{ (MPa)} \quad (13)$$

where: σ_t is the tension stress; ε_c is concrete strain taken as 0.05.

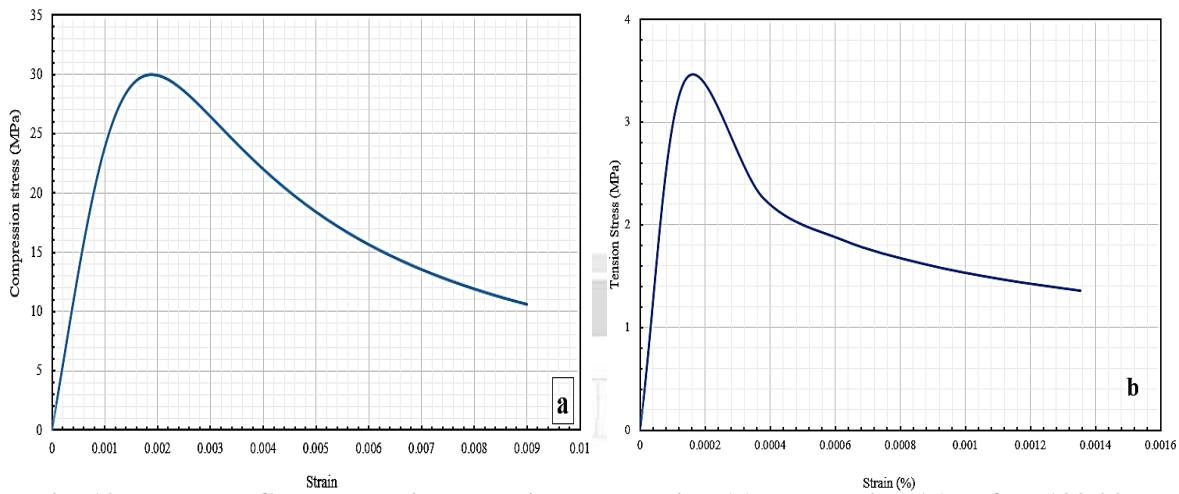


Fig. 10: The UHPC stress-strain curve, in compression (a) and tension (b) at $f_c = 132.02$ MPa.

This method for UHPC tension response is devised by Shafieifar et al. in 2017 [24].

The elastic-perfect plastic approach is used to model the materials of reinforcing steel bars, as shown in Fig. 11. For all reinforcing bars, the initial tangent modulus of elasticity (E_s) and Poisson's ratio (ν_s) are given as 200 GPa and 0.3, respectively, to denote the elastic phase [25].

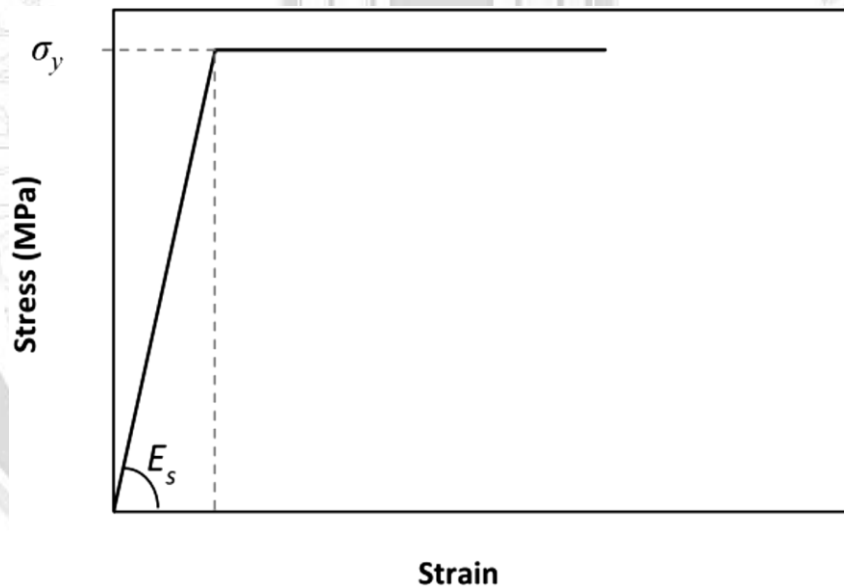


Fig. 11: Steel reinforcing stress-strain curve [26].

The components' interaction was established using the following methodology: an embedded constraint was applied between the steel reinforcement and concrete, a surface-to-surface contact was applied between precast concrete and cast-in-place UHPC, and a tie constraint was used for the plate load and support on the concrete surface. The friction coefficient for this contact was adjusted to 1.44 and it was characterized as "hard contact" in

the tangent direction. A "penalty" technique was employed[23,27]. These principles were consistently applied to other types of strengthening materials.

The load-deflection response and mode of failure of the beams (CB, BT, RU, and NGb) that were validated in this study showed good agreement with experimental results. Table 7 summarizes the information, and Figs. 12 through 19 provide illustrations. Small discrepancies in performance could be explained by changes in boundary conditions between the finite element (FE) model and the experimental specimens. For instance, the FE modeling did not account for the friction between the loading plates and the specimens. It is important to stress that the main goal of the modeling was to define a hybrid material that complies well with test specimen experimental data. Reaching an ideal fit for every outcome proved unachievable. It is also critical to understand that test results can be influenced by a number of variables, including the age of the concrete and the fiber amount.

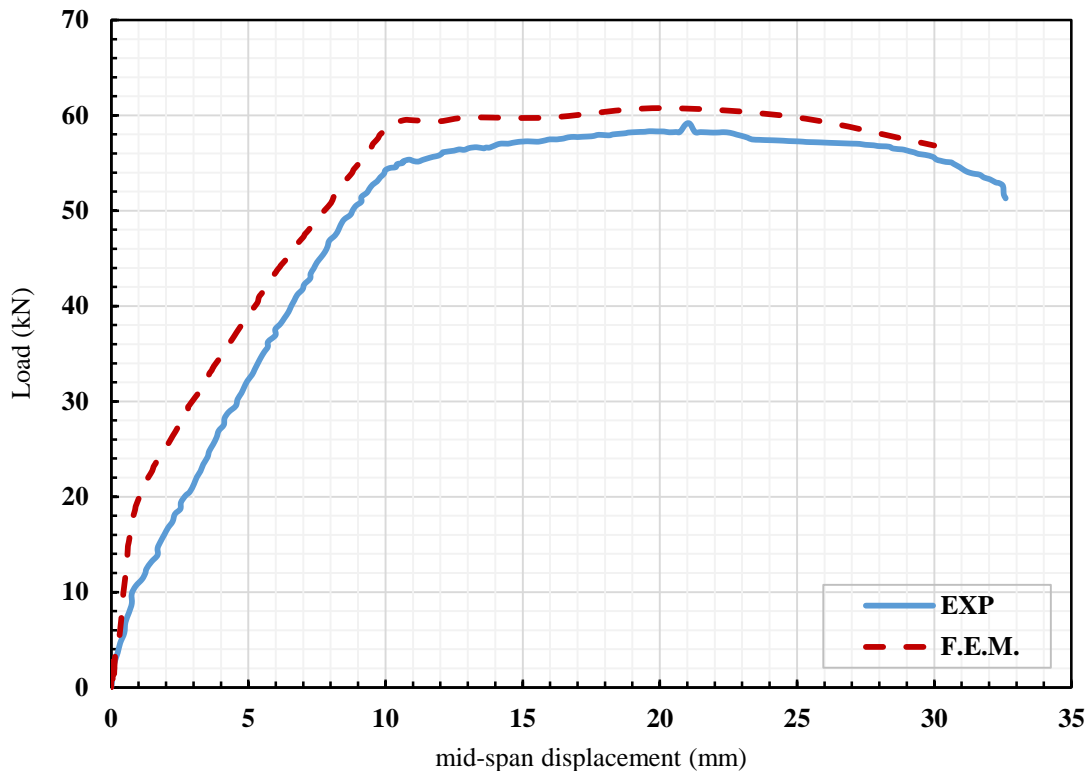


Fig. 12: Load- mid-span deflection relationship of CB.

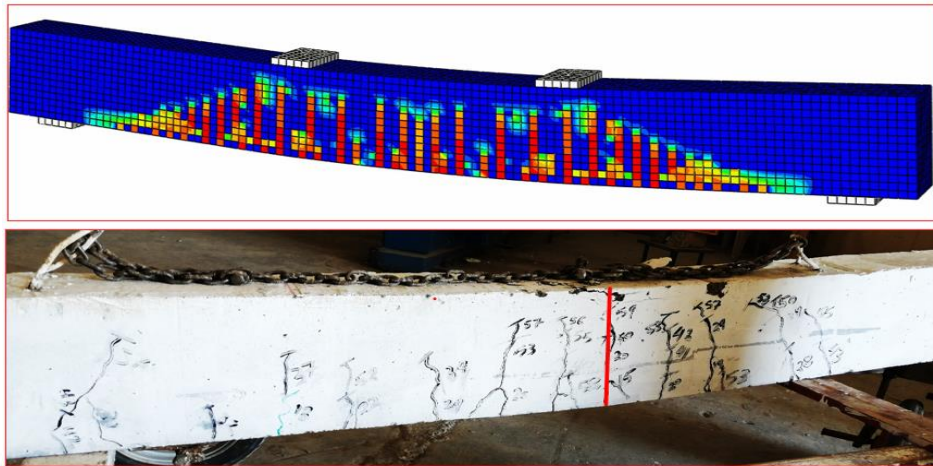


Fig. 13: Crack pattern of CB.

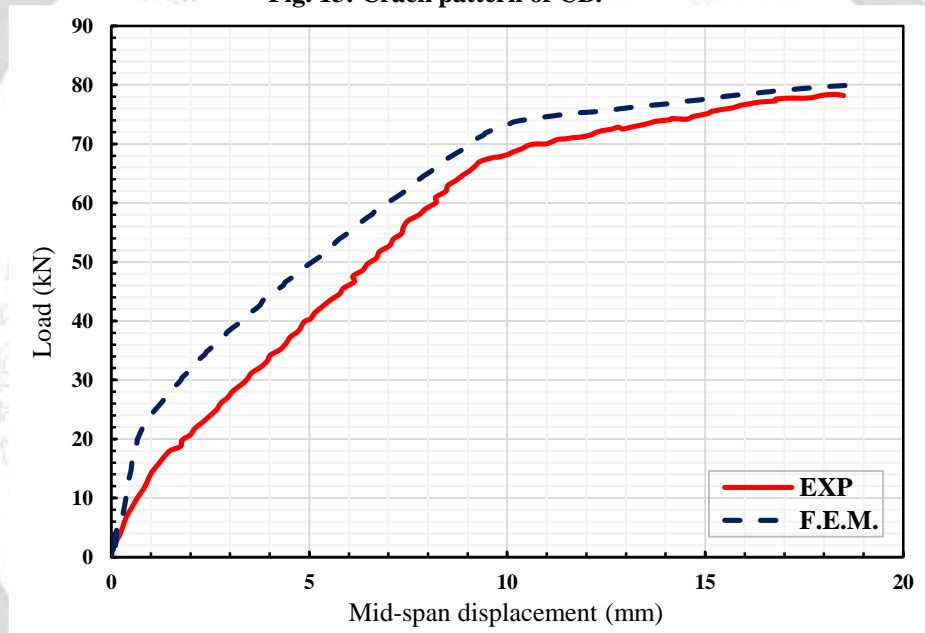


Fig. 14: Load- mid-span deflection relationship of BT.

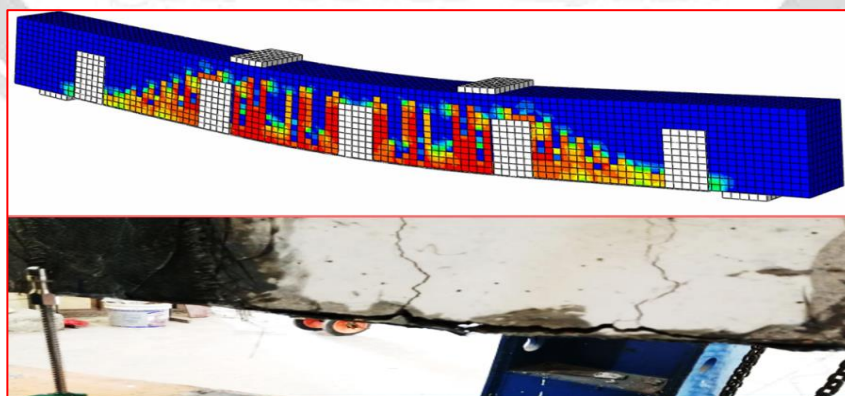


Fig. 15: Crack pattern of BT.

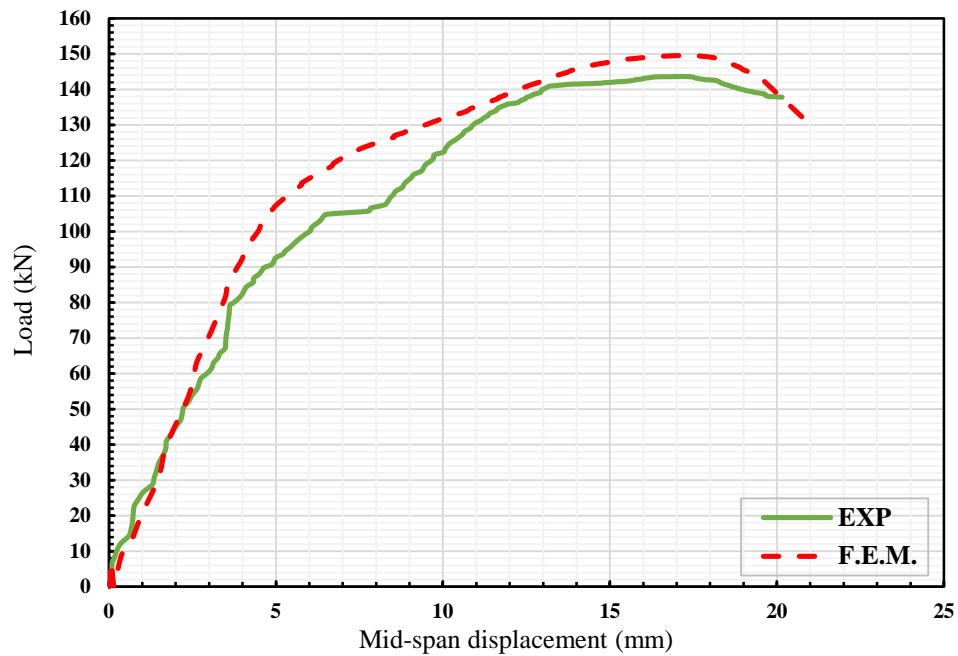


Fig. 16: Load- mid-span deflection relationship of RU.

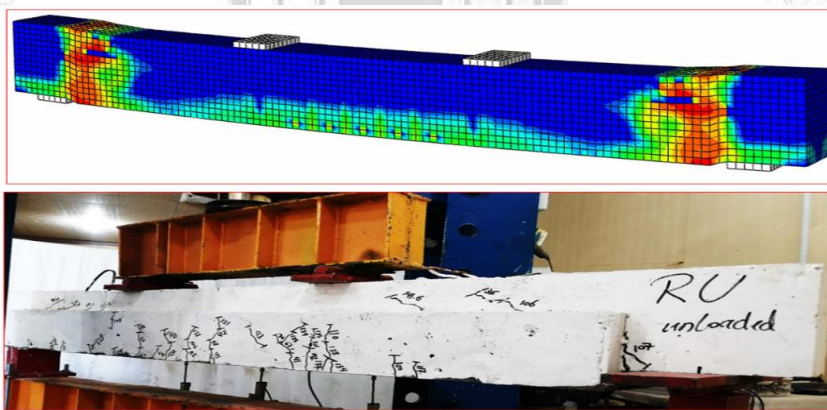


Fig. 17 a: Crack pattern of RU.



Fig. 17 b: Crack pattern of RU.

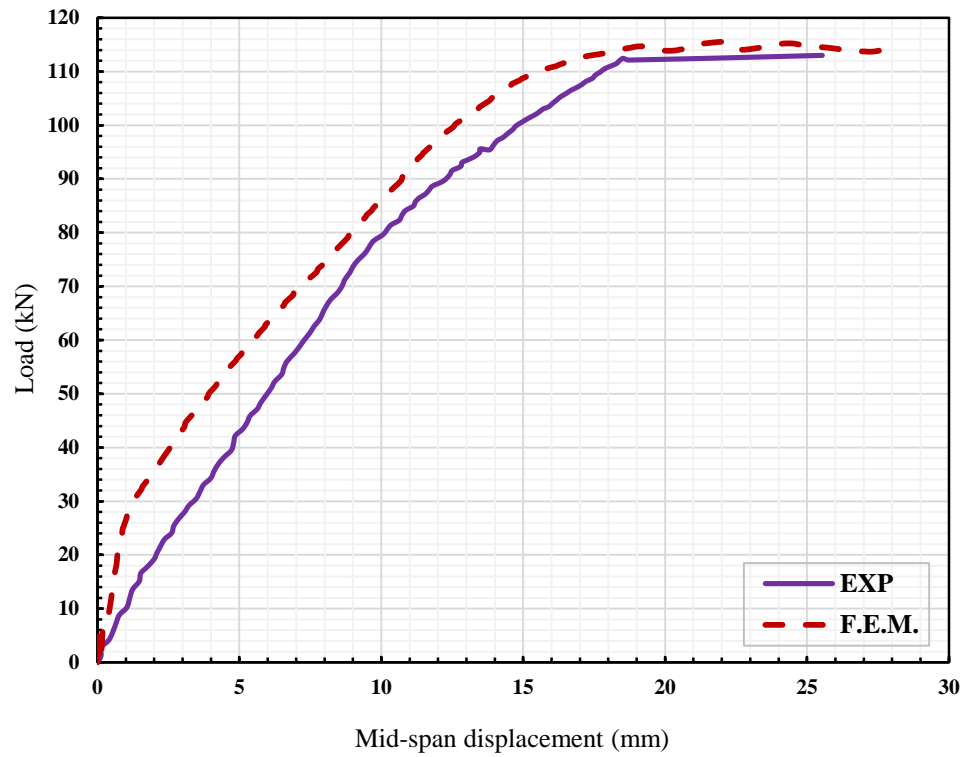


Fig. 18: Load- mid-span deflection relationship of NGb.

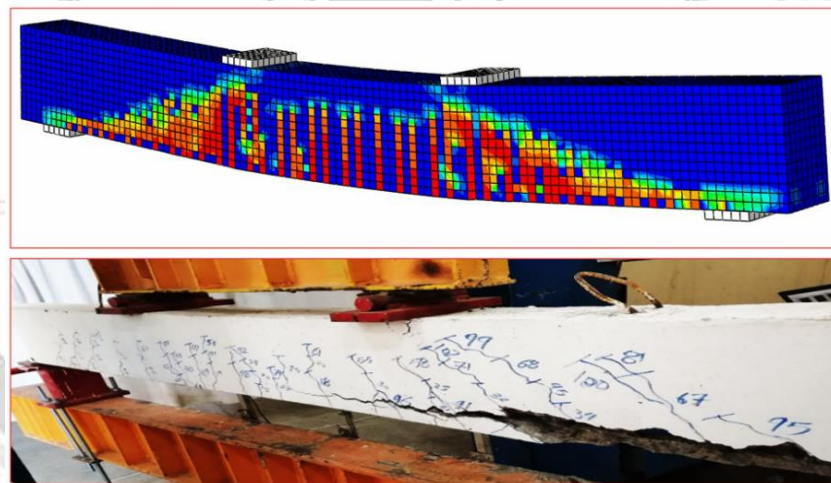


Fig. 19: Crack pattern of NGb.

Table 7: Results of validation for the analyzed beams.

Specimen	Pu _{exp.} (kN)	Pu _{Num.} (kN)	Pu _{exp./Pu_{Num.}}	Δu _{exp.} (mm)	Δu _{Num.} (mm)	Δu _{exp./Δu_{Num.}}
CB	59.12	59.53	0.993	29.82	21.25	1.40
BT	78.34	80.03	0.978	18.31	18.85	0.971
RU	143.65	149.58	0.960	17.19	17.19	1
NGb	112.93	114.68	0.985	18.73	19.11	0.980

5. Conclusion

The performance of a reinforced concrete beam strengthened with BFRP (BT), R-UHPC (RU), and NSM-GFRP (NGb) is the main focus of this experimental investigation. To investigate the effects of various strengthening types on the structural behavior, four specimens were used. The study explores the formation of cracks, the manner of failure, the ultimate load, and the specimens' reaction to load deflection. The following is a summary of the study's main conclusions:

- 1- A significant enhancement in the ultimate load capacity was observed for all reinforced beams in comparison to the control beams.
- 2- The cracks were concentrated in the mid-span zone, and flexural failure was predominant in all beams.
- 3- Before flexural cracking, the load-deflection response behaved linearly; after that, differences in the beam yielding stages were visible. Good ductile responses were shown by all beams prior to the collapse stage.
- 4- The reinforced beams displayed a substantial percentage increase in loading capacity, with increments of (32%, 143%, and 91%) for beams strengthened with BFRP (BT), R-UHPC (RU), and NSM-GFRP (NGb) respectively, when compared to the control beams.
- 5- The ultimate capacity of RU enhanced is more than that of the other materials employed in this paper (BT, and NGb).
- 6- The experimental findings were used to implement and evaluate the finite element (FE) model, and the results showed a good agreement with respect to the mode of failure and the load-deflection response.

The main objective of this research is to evaluate the influence of different strengthen materials on beam strengthening in the flexural zone.

Acknowledgements:

The specimens underwent testing at University of Babylon in Civil Engineering Department structural laboratory. The authors extend sincere appreciation and admiration to this establishment. Gratitude is extended to all friends who provided assistance and encouragement in completing this effort.

Author contributions:

Waleed Hamed Kamel: Methodology, Investigation, Writing – original draft, Writing - review & editing, Visualization, Formal analysis, Validation. **Bilal Ismaeel Abd Al-Zahra:** Methodology, Supervision, Leadership, Reading, Editing.

Funding:

This manuscript was prepared without the assistance of any funding.

Declarations:

Conflict of Interest Declaration: The author(s) has declared that there are no possible conflicts of interest pertaining to the study, writing, or distribution of this work.

6. Reference

- [1] M. Ozakça Asaad M. H. Kadhim , Hesham A. Numan, “Flexural Strengthening and Rehabilitation of Reinforced Concrete Beam Using BFRP Composites: Finite Element Approach.” p. 17, 2019.
- [2] M. P. J. Mr.Ankit .U. Oza, “Experimental study on Retrofitting of RC beam using Basalt Fibers.” p. 8, 2017.
- [3] S. B. W. Harshwardhan Surwase, G. N. Narule, “Behavior of RC T-Beam Strengthen Using Basalt Fiber Reinforced Polymer (FRP) Sheet.” p. 6, 2019.
- [4] M. Y. G.Viswanathan, G.Oviya, A.Sabitha priyadharshini, K.R.Santhiya, “EXPERIMENTAL STUDY ON STRENGTHENING OF RC BEAM USING FIBRE WRAPPING.” p. 7, 2019.
- [5] M. Alkaysi and W. H. , Sherif El-Tawil, Zhichao Liu, “Effects of silica powder and cement type on durability of ultra high performance concrete (UHPC).” p. 10, 2016.
- [6] J. Qi, Z. J. Ma, and J. Wang, “Shear Strength of UHPFRC Beams: Mesoscale Fiber-Matrix Discrete Model,” *Journal of Structural Engineering*, vol. 143, no. 4. p. 10, 2017. doi: 10.1061/(asce)st.1943-541x.0001701.
- [7] B. H. A. B. Bassam A. Tayeh , Mahmoud H. Akeed , Shaker Qaidi, “Ultra-high-performance concrete: Impacts of steel fibre shape and content on flowability, compressive strength and modulus of rupture.” p. 7, 2022.
- [8] B. Graybeal, “Bond of Field-Cast Grouts to Precast Concrete Elements.” p. 19, 2017. [Online]. Available: www.fhwa.dot.gov/research
- [9] B. A. Graybeal, “Design and Construction of Field-Cast UHPC Connections: TECHNNOTE,” *Fhwa-Hrt-14-084*, no. October. pp. 1–36, 2014. [Online]. Available: <https://www.fhwa.dot.gov/publications/research/infrastructure/structures/14084/14084.pdf>
- [10] C. Roberto, “On the strengthening of RC beams with near surface mounted GFRP rods,” *Composite Structures*, vol. 117, no. 1. pp. 143–155, 2014. doi: 10.1016/j.compstruct.2014.06.030.
- [11] H. Y. L. W.C. Tang, R.V. Balendran, A. Nadeem, “Flexural strengthening of reinforced lightweight polystyrene aggregate concrete beams with near-surface mounted GFRP bars.” p. 13, 2005.
- [12] R. M. Reda, I. A. Sharaky, M. Ghanem, M. H. Seleem, and H. E. M. Sallam, “Flexural behavior of RC beams strengthened by NSM GFRP Bars having different end conditions,” *Composite Structures*, vol. 147. pp. 131–142, 2016. doi: 10.1016/j.compstruct.2016.03.018.

- [13] H. El-Emam, A. El-Sisi, R. Reda, S. Mohamed, and BneniMohamed, "Effect of concrete cover thickness and main reinforcement ratio on flexural behavior of RC beams strengthened by NSM-GFRP bars," *Frattura ed Integrita Strutturale*, vol. 14, no. 52. pp. 197–210, 2020. doi: 10.3221/IGF-ESIS.52.16.
- [14] (2019) 318M-19 ACI 318-19, "Building Code Requirements for Structural Concrete and Commentary." p. 628, 2019.
- [15] ASTM C1856, "Standard Practice for Fabricating and Testing Specimens of Ultra-High Performance Concrete." 2017. doi: <https://doi.org/10.1520/C1856>.
- [16] M. I. Yuliarti Kusumawardaningsih, Ekkehard Fehling, "UHPC compressive strength test specimens: Cylinder or cube?" by Elsevier Ltd, p. 5, 2015. doi: Peer-review under responsibility of organizing committee.
- [17] B. G. and M. Davis, "Cylinder or Cube: Strength Testing of 80 to 200 MPa (11.6 to 29 ksi) Ultra-High-Performance Fiber-Reinforced Concrete." p. 7, 2008.
- [18] O. Q. A. & G. H. Ahmed, "Mechanical Properties of Ultra High Performance Concrete (UHPC)." pp. 331–346, 2012.
- [19] ASTM C469-11, "Standard test method for splitting tensile strength of cylindrical concrete specimens. Manual on Hydrocarbon Analysis." p. 5, 2008.
- [20] I. K. H. and A. Y. A. Wissam Nadir, "Optimization of ultra-high-performance concrete properties cured with ponding water." p. 18, 2022.
- [21] J. P. B. S. Sami H. Rizkalla Chai, "Guide Test Methods for Fiber-Reinforced Polymers (FRPs) for Reinforcing or Strengthening Concrete Structures." p. 40, 2004.
- [22] T. T. . H. Taijun Wang, "Nonlinear finite element analysis of concrete structures using new constitutive models." pp. 2781–2791, 2001.
- [23] Graybeal and Russell, "Ultra-High Performance Concrete: A State-of-the-Art Report for the Bridge Community." p. 176, 2013.
- [24] A. A. Shafieifar Mohamadreza , Mahsa Farzad, "Experimental and numerical study on mechanical properties of Ultra High Performance Concrete (UHPC)." pp. 402–411, 2017.
- [25] A. H. A. A.-A. Zainab Kareem Al-Mamory, "Behavior of steel fiber reinforced concrete beams with CFRP wrapped lap splice bars." pp. 1995–2011, 2022. doi: 10.1016/j.istruc.2022.08.096.
- [26] M. M. A. Kadhim, A. R. Saleh, and A. A. S. , Lee S. Cunningham, "Numerical investigation of non-shear-reinforced UHPC hybrid flat slabs subject to punching shear." p. 50, 2021.
- [27] Q. Zhang, Y. Feng, Z. Cheng, Y. , Jiao, H. Cheng, and J. W. and J. Qi, "Large-scale testing and numerical study on an innovative dovetail UHPC joint subjected to negative moment." pp. 175–183, 2022.

**تقوية الاعتاب الخرسانية المسلحة في منطقة الانثناء باستخدام مواد مختلفة: دراسة
تجريبية وعددية**وليد حامد كامل¹ بلال إسماعيل عبد الزهرة²¹هندسة مدنية، كلية الهندسة، جامعة بابل، الحلة- بابل- العراق.waleed.omran.engh323@studen.uobabylon.edu.iq²كلية الهندسة، جامعة بابل، الحلة- بابل- العراق.eng.bilal.ismaeel@uobabylon.edu.iq**الخلاصة**

يُعتقد أن العوارض التي تتشقق يتم تقويتها بشكل أسرع باستخدام مواد التقوية. الغرض من هذه الدراسة هو التحقق من كيفية تصرف الخرسانة فائقة الأداء (R-UHPC)، والبوليمر المقوى بالألياف البازلتية (BFRP)، وقضيب البوليمر المقوى بالألياف الزجاجية المثبتة على السطح القريب (NSM-GFRP) في الخرسانة المسلحة ذات الاسناد البسيط. لإكمال هذه الدراسة، كان لابد من إعداد أربع عوارض، وصيها، واختبارها. حيث تم اعتماد إحدى العوارض كعارضة تحكم، وتم تقوية العوارض الثلاث المتبقية بثلاثة أنواع مختلفة من التقوية سيتم شرحها لاحقاً. ومن متغيرات الدراسة شكل أو نوع التقوية. لاختبار العينات، طبقت التقنية المحددة حملاً من نقطتين. من خلال الاختبارات والحصول على الحمل النهائي، طريقة الفشل، تطور التشقق، واستجابة العلاقة بين الحمل- الهطول، تمت دراسة السلوك الهيكلي للعينات. أوضحت نتائج الدراسة أنه بالمقارنة مع عارضة التحكم والعوارض المقواة، فإن العارضة المقواة بـ R-UHPC أعطت زيادة كبيرة في الحمل النهائي. حيث تم تحسين الحمل النهائي بنسبة 143% في عينات R-UHPC، و 32.5% في عينات BFRP، و 91.01% في عينات NSM-GFRP عند وجود التقوية. بالإضافة إلى ذلك، تم إجراء التحليل العددي باستخدام ABAQUS على النماذج المتوقعة للعوارض المختبرة تجريبياً. أظهرت استجابة انحراف الحمل وآلية الفشل توافق نتائج نموذج F.E مع الاختبار العملي بشكل جيد.

الكلمات الدالة:- تقوية، BFRP, R-UHPC, and NSM-GFRP